Experimental and numerical evidence for intrinsic nonmigrating bars in alluvial channels

Alessandra Crosato,[1,2] Erik Mosselman,[1,3] Frehiwot Beidmariam Desta,[2,4] and Wim S. J. Uijttewaal[5]

Received 2 July 2010; revised 15 December 2010; accepted 4 January 2011; published 8 March 2011.

[1] Alternate bars in straight alluvial channels are migrating or nonmigrating. The currently accepted view is that they are nonmigrating if the width-to-depth ratio is at the value of resonance or if the bars are forced by a persistent local perturbation. We carried out 2-D numerical computations and a long-duration mobile-bed flume experiment to investigate this view. We find that nonmigrating bars can also occur in straight channels without resonant width-to-depth ratio or steady local perturbation. They appear to be an intrinsic response of the alluvial river bed. This finding bears on explanations for meandering of alluvial rivers, for which nonmigrating bars are seen as a prerequisite. We find, however, that the intrinsic tendency of a straight channel to form meanders usually has a different origin. The identified intrinsic nonmigrating bars can only become the dominant mechanism for incipient meandering if the erodibility of the banks is very low.

Citation: Crosato, A., E. Mosselman, F. Beidmariam Desta, and W. S. J. Uijttewaal (2011), Experimental and numerical evidence for intrinsic nonmigrating bars in alluvial channels, *Water Resour. Res., 47*, W03511, doi:10.1029/2010WR009714.

1. Introduction

[2] Alternate bars in alluvial channels can be migrating or nonmigrating. Both forms are natural free responses of the system of water flowing over a mobile sediment bed, but nonmigrating alternate bars tend to dominate in rivers with arbitrary planforms, whereas migrating alternate bars are common in straight alluvial channels with a uniform width. It is usually assumed that alternate bars in straight alluvial channels with a constant discharge can be nonmigrating only if the width-to-depth ratio is at the value of resonance or if the bars are forced by a persistent local perturbation [e.g., *Blondeaux and Seminara*, 1985; *Olesen*, 1984; *Struiksma et al.*, 1985; *Tubino and Seminara*, 1990]. Here we investigate the possibility that nonmigrating bars can also become dominant spontaneously in straight alluvial channels without these prerequisites.

[3] Nonmigrating alternate bars arouse specific interest because they are closely related to the formation of meanders. River meandering has intrigued generations of researchers, including Leonardo da Vinci [e.g., *Macagno*, 1989] and Albert Einstein [*Einstein*, 1926]. Natural rivers usually develop a windy course because of irregularities in the terrain, but despite the randomness of those irregularities, they often evolve into regular meander geometries. Yet more intriguing is that initially straight alluvial channels with uniform characteristics develop into meandering courses. Up to the 1970s, this was even called "mysterious" [e.g., *Lebreton*, 1974]. Some researchers proposed that meandering resulted from an inherent instability of the system of water and sediment motion, potentially understood from a stability analysis, but others invoked earth rotation or extremal hypotheses to explain the onset of meandering.

[4] Stability analyses were carried out in the 1970s and 1980s. Two distinct approaches emerged: a bar theory and a bend theory. The *bar theory* considers the stability of the alluvial bed and shows that this bed may develop into a pattern of alternate bars [e.g., *Hansen*, 1967; *Callander*, 1969; *Engelund and Skovgaard*, 1973; *Parker*, 1976; *Fredsøe*, 1978]. Different bar wavelengths may be unstable, but according to the theory the wavelength selected corresponds to the bars with the largest temporal growth rate. At the pools between these bars, near-bank flow velocities and water depths are higher and may thus give rise to localized bank erosion, transforming an initially straight channel into a sinuous one. The *bend theory* [*Ikeda et al.*, 1981] considers the planform stability of a straight channel and shows that an infinitesimal perturbation of the channel centerline may lead to the development of meanders. It assumes the presence of bars implicitly through a relation between local channel curvature and cross-sectional bed level asymmetry.

[5] The problem was that the resulting bar wavelength according to the bend theory was much larger than the wavelength of alternate bars with fastest growth according to the bar theory. *Olesen* [1984] argued, however, that the alternate bars with the largest growth rate are migrating so fast that they lead to uniform bank erosion rather than localized bank erosion if the banks are not highly erodible (Figure 1). The result is channel widening rather than channel meandering. Olesen proposed that nonmigrating alternate bars offer a more adequate explanation for the

[1]Section of Hydraulic Engineering, Faculty of Civil Engineering and Geosciences, Delft University of Technology, Delft, Netherlands.
[2]UNESCO-IHE, Delft, Netherlands.
[3]Deltares, Delft, Netherlands.
[4]Ethiopian Road Authority, Addis Ababa, Ethiopia.
[5]Section of Fluid Mechanics, Faculty of Civil engineering and Geosciences, Delft University of Technology, Delft, Netherlands.

Copyright 2011 by the American Geophysical Union.
0043-1397/11/2010WR009714

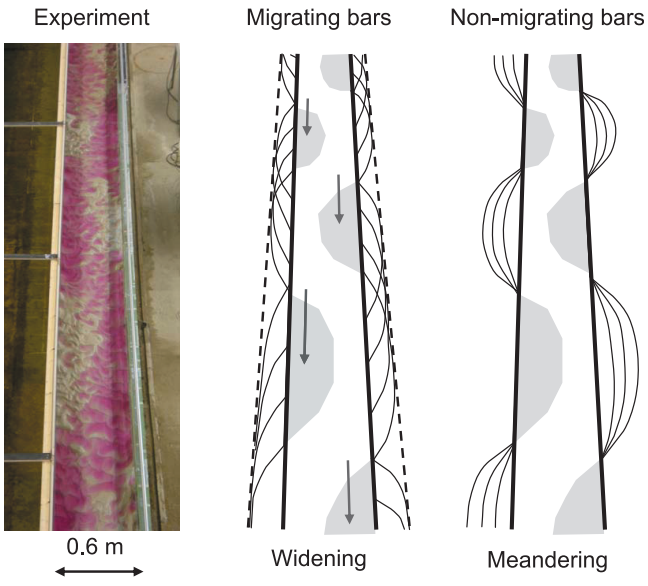

Figure 1. (left) Experimental flume looking from downstream. Alternate bars become visible with colored water. (middle) If bars are migrating and banks are erodible, the channel tends to widen. (right) If bars are nonmigrating and banks are erodible, the channel starts to meander. The drawing aims at describing the concept, but does not aim at showing the complex process of meander formation.

formation of meanders. First, they are a condition for localized bank erosion. Second, this localized bank erosion produces incipient meanders and associated curvature driven point bars with the same wavelength. This leads to a form of self-excitation in the incipient meanders, because bars forced by channel curvature excite the natural wavelength of the nonmigrating bars responsible for the bank erosion that curves the channel. *Olesen* [1984] and *De Vriend and Struiksma* [1984] argued that, in the absence of channel curvature, nonmigrating bars can be forced by a persistent local perturbation, such as a local variation in channel geometry. This can be a local groyne, but also the result of localized bank erosion by a migrating bar within a time frame shorter than the bar wave period. The uniform widening in Figure 1 is hence an idealized picture for the sake of argument. Initial localized erosion because of migrating bars causes a bankline variation which forces a nonmigrating bar pattern over some distance downstream. The growth of meanders is then transmitted from upstream to downstream. *Struiksma et al.* [1985] presented a linear model for these nonmigrating bars by setting migration rate and temporal growth rate equal to zero. This model for marginally stable nonmigrating bars agreed well with laboratory and field observations and produced similar wavelengths as the bend theory. *Seminara and Tubino* [1992] found the same marginally stable nonmigrating bars in their theoretical analysis.

[6] *Blondeaux and Seminara* [1985] presented another linear model by setting the spatial growth rate equal to zero, which corresponds to considering only alternate bars with constant amplitude along the channel. They discovered resonance in the resulting system at vanishing bar migration rates and vanishing temporal growth rates. They proposed that this resonance might explain the selection of nonmigrating bars and the onset of meandering at larger wavelengths than the wavelengths of migrating alternate bars with maximum temporal growth rate. Contrary to *Olesen*'s [1984] self-excitation of nonmigrating bars by incipient meanders of the same wavelength, this resonance occurs only at a specific width-to-depth ratio, because the wavelength of the corresponding nonmigrating bar is a function of this width-to-depth ratio. Under this particular condition, meanders grow simultaneously and uniformly along the entire channel.

[7] *Parker and Johannesson* [1989] demonstrated that the nonmigrating-bar model of *Struiksma et al.* [1985] exhibits resonance as well. This model, based on equating temporal growth rates to zero beforehand, exhibits resonance at vanishing spatial growth rates, whereas the nonmigrating-bar model of *Blondeaux and Seminara* [1985], based on equating spatial growth rates equal to zero beforehand, exhibits resonance at vanishing temporal growth rates. Indeed, both models predict resonance at the same wavelength and channel width-to-depth ratio. Both models allow a distinction between subresonant, resonant, and super-resonant conditions. Width-to-depth ratios larger than the resonant value pertain to super-resonant conditions in both cases, but this is because of positive spatial growth rates in the model of *Struiksma* et al. [1985] and because of positive temporal growth rates in the model of *Blondeaux and Seminara* [1985]. Despite differences in the details, the explanations based on stability analysis found wide support, as they were based on validated physical concepts of water and sediment motion [cf. *Rhoads and Welford*, 1991].

[8] Experimentally, both widening until the resonant width-to-depth ratio and a persistent perturbation had been shown to produce the nonmigrating bars that are needed to explain the onset of river meandering [*Fujita and Muramoto*, 1982; *Struiksma and Crosato*, 1989]. The question remained, however, whether nonmigrating bars can also be an intrinsic response of an alluvial channel bed in straight channels, without external forcings or resonant conditions.

[9] Other research refined the picture. Nonmigrating bars can coexist with migrating bars, but they were found to suppress migrating bars at larger channel sinuosity [*Kinoshita and Miwa*, 1974; *Tubino and Seminara*, 1990] and at greater channel slope [*Lisle et al.*, 1991]. Flume experiments by *Fujita and Muramoto* [1985], as reported by *Nelson and Smith* [1989], showed that migrating alternate bars become slower and longer as they develop toward a finite amplitude. Nonlinear computations by *Nelson* [1990] confirmed the bar elongation. This reduced the gap between the short migrating alternate bars that grow fastest and the long nonmigrating alternate bars needed for the onset of meandering, although it did not bridge the gap fully. *Hall* [2004] found from a weakly nonlinear stability analysis of unsteady flow that interaction of discharge variations and migrating alternate bars produced a nonmigrating sinusoidal structure of the bed, which he suggested to be relevant to meander formation. However, the discharge variations can still be seen as an external forcing and meanders are known to form at constant discharge as well.

[10] Notwithstanding these refinements, the general theoretical picture remained that nonmigrating bars and incipient meandering require a resonant width-to-depth ratio, a persistent perturbation, or, possibly, a variable discharge.

We performed a series of numerical tests and a laboratory experiment to investigate bar formation in a straight flume with mobile bed without any persisting perturbations and with constant discharge at nonresonant conditions.

[11] Section 2 presents the numerical simulations for long durations using a physics-based depth-averaged nonlinear numerical model. Here short migrating alternate bars developed first, but slowly growing nonmigrating bars, characterized by larger wavelengths, evolved subsequently, starting from either upstream or downstream. The nonmigrating bars tended to dominate the final bed topography.

[12] Section 3 describes the long-duration laboratory experiment. Here migrating bars developed first too. In a test without external forcing, the first nonmigrating bar stabilized its length about 3 weeks after the start of the experiment. Subsequently, this bar grew slightly in amplitude and two more nonmigrating bars became visible about 6 weeks after the start of the experiment. Again, nonmigrating bars tended to dominate the final bed topography.

[13] Section 4 reviews earlier experiments on migrating alternate bars where either a steady oscillation or bars with a similar wavelength to nonmigrating bars had been observed. These nonmigrating bars were previously ascribed to imperfections in the uniformity of the inflow conditions, but our findings suggest that they could have been an intrinsic response of the alluvial river bed. As nonmigrating bars are seen as a key ingredient in explanations of river meandering, we also reviewed mobile-bed experiments with erodible banks. Here meanders developed without a steady upstream perturbation or resonant conditions, most likely triggered, however, by initial localized bank erosion because of migrating alternate bars instead of the development of intrinsic nonmigrating bars.

[14] We conclude that both nonmigrating alternate bars in straight channels with nonerodible banks and incipient meanders in straight channels with erodible banks are intrinsic responses of an alluvial channel bed that do not require resonant conditions or an imposed steady upstream perturbation. However, the nature of the two intrinsic responses is different. We argue, nonetheless, that the slow development of intrinsic nonmigrating bars may still become the main mechanism for incipient meandering if the erodibility of the banks is very low.

2. Numerical Tests

2.1. Model Setup

[15] We simulated the formation of bars in straight alluvial channels using a fully nonlinear, time-dependent, physics-based numerical model for morphological processes [*Lesser et al.*, 2004]. The hydrodynamic part of the model is based on the 3-D Reynolds-averaged Navier–Stokes (RANS) equations for incompressible fluid and water (Boussinesq approximation). We used a 2-D depth-averaged version of the model with an appropriate parametrization of two relevant 3-D effects of the spiral motion that arises in curved flow [cf. *Blanckaert et al.*, 2003]. First, the model corrects the direction of sediment transport through a modification in the direction of the bed shear stress, which would otherwise coincide with the direction of the depth-averaged flow velocity vector. Second, the model includes the transverse redistribution of main flow velocity because of secondary-flow convection, through a correction in the bed friction term. The closure scheme for turbulence is a $k-\varepsilon$ model, in which k is the turbulent kinetic energy and ε is the turbulent dissipation.

[16] The evolution of bed topography is computed from a sediment mass balance and a sediment transport formula. The model accounts for the effects of gravity along longitudinal and transverse bed slopes on bed load direction [*Bagnold*, 1966; *Ikeda*, 1982].

[17] The equations are formulated in orthogonal curvilinear coordinates. The set of partial differential equations in combination with the set of initial and boundary conditions is solved on a finite difference grid.

[18] We simulated the evolution of bed topography in straight river channels with uniform width and nonerodible banks. The banks were fixed in order to avoid any external forcing of the flow arising from geometrical changes of the river banks. We ran two cases with different channel width-to-depth ratios and discharges. Sediment characteristics and longitudinal bed slope were loosely based on the Waal River in the Netherlands. The other characteristics were selected such that both nonmigrating and migrating alternate bars could be formed. We defined the range of width-to-depth ratios suitable for the formation of migrating alternate bars by using results of *Marra* [2008], who applied *Tubino and Seminara*'s [1990] method to the Waal River. Suitable ranges for the formation of nonmigrating alternate bars were determined by selecting $m = 1$ in the physics-based formula of *Crosato and Mosselman* [2009]:

$$m^2 = 0.17g\frac{(b-3)}{\sqrt{\Delta D_{50}}}\frac{B^3 S}{C Q_W}, \tag{1}$$

in which m is the bar mode, b is the degree of nonlinearity in the relation between sediment transport rate and depth-averaged flow velocity, B is the channel width, S is the longitudinal channel gradient or bed slope, Δ is the relative submerged mass density of the sediment, D_{50} is the median grain size, C is the Chézy coefficient for hydraulic resistance, and Q_W is the water discharge. The degree of nonlinearity is equal to the exponent in case of a power law dependence $q_s \propto u^b$ and is always larger than 3 [e.g., *Mosselman*, 2005]. We kept the width-to-depth ratios well below 100 to remain within the validity range of equation (1).

[19] The length of the channel was 20 km; the longitudinal bed slope 10^{-4} (0.1 m/km). The roughness coefficient C_f, was assumed constant in space and time, with the value of 0.005. The sediment was assumed uniform with a grain diameter of 2 mm and relative submerged mass density of 1.65 (from a sediment mass density of 2650 kg/m^3). The sediment transport rates were computed using *Engelund and Hansen*'s [1967] formula, valid for sand-bed rivers. The sediment input at the upstream boundary was computed with the same formula, which means that the input from upstream was equal to the local sediment transport capacity of the flow. The other channel characteristics are summarized in Table 1.

[20] The conditions with respect to resonance can be derived following the simplified linear approach by *Struiksma et al.* [1985], i.e., by computing the longitudinal damping coefficient of nonmigrating bars $1/L_D$. At resonance, this coefficient is equal to 0; the system is

Table 1. Characteristics of the Simulated Alluvial Rivers

Variable	RUN1	RUN2
Q_W (m^3/s)	200	300
B (m)	90	150
h_0 (m)	3.0	2.8
B/h_0 (-)	30	53
Nonmigrating bars m (-)[a]	1	1
Migrating bars m (-)[b]	1	1–2
Groyne length (m)[c]	30	20

[a]Mode according to *Crosato and Mosselman* [2009].
[b]Mode according to *Marra* [2008].
[c]Reference runs.

subresonant if $1/L_D$ has a positive value, the system is super-resonant if $1/L_D$ is negative. The formula used is the following:

$$\frac{1}{L_D} = \frac{1}{2\lambda_w}\left(\frac{\lambda_w}{\lambda_s} - \frac{b-3}{2}\right), \tag{2}$$

where

$$\lambda_W = \frac{h_0}{2C_f}, \tag{3}$$

$$\lambda_s = \frac{1}{\pi^2} h_0 \left(\frac{B}{h_0}\right)^2 f(\theta_0), \tag{4}$$

in which h_0 is the reach-averaged water depth, C_f is the friction factor defined by $C_f = \frac{g}{C^2}$, in which g is the acceleration because of gravity, and $f(\theta_0)$ accounts for the effect of gravity on the direction of sediment transport over transverse bed slopes. It satisfies an empirical relation [*Talmon et al.*, 1995]:

$$f(\theta_0) = \frac{0.85}{E}\sqrt{\theta_0}, \tag{5}$$

where E is a calibration coefficient with a value around 0.5 and θ_0 is the reach-averaged value of the Shields parameter.

[21] The wavelength L_P of nonmigrating bars can be computed as follows [*Struiksma et al.*, 1985]:

$$\frac{2\pi}{L_P} = \frac{1}{\lambda_w}\left(\frac{\lambda_w}{\lambda_s} - \left(\frac{\lambda_w}{L_D}\right)^2\right)^{1/2}. \tag{6}$$

[22] Table 2 lists the damping coefficient (equation (2)) and the wavelength (equation (6)) of nonmigrating bars derived from the linear model by *Struiksma et al.* [1985], assuming $b = 5$ (*Engelund and Hansen*'s [1967] transport formula) and $E = 0.5$.

[23] The numerical parameters of the model setup are summarized in Table 3. The morphological factor in Table 3 amplifies the bed level changes in each hydrodynamic time step to reduce the computational time for morphological development. It serves as the ratio between morphological and hydrodynamic time steps. This factor was given the largest possible value that still kept the simulations realistic. Nonetheless, even with a morphological factor equal to 10, some runs took more than 40 days real time for completion. Sensitivity analyses showed that the bar celerity increased for increasing morphological factor. The minor overestimation of bar celerity when using a morphological factor equal to 10 was considered an acceptable shortcoming, since the focus of the study was on the stabilization of migrating bars.

Table 2. Damping Coefficient and Wavelength of Nonmigrating Bars Computed According to the Linear Model by *Struiksma et al.* [1985]

Variable	RUN1	RUN2
$1/L_D$ (m^{-1})	0.002	−0.001
Wavelength nonmigrating bars (m)	1332	2073

[24] The reproduction of migrating bars in a numerical model requires an unsteady forcing at the upstream boundary [e.g., *Struiksma*, 1998; *Mosselman et al.*, 2003]. For this reason, a very small, randomly varying perturbation of the inflow was distributed in transverse direction over the computational grid cells at the upstream boundary. We applied two different magnitudes and frequencies of the perturbation: (1) maximum amplitude equal to 1% of the discharge, varying every minute (simulated hydrodynamic time); and (2) maximum amplitude equal to 5% of the discharge, varying every 3.5 h (simulated hydrodynamic time). We also carried out simulations with a permanent finite perturbation at the upstream boundary, similar to the presence of a groyne obstructing part of the channel width. These simulations provided reference conditions to assess the characteristics of the nonmigrating bars that are known to form downstream of steady local perturbations [*Struiksma and Crosato*, 1989; *Lanzoni*, 2000a]. The downstream boundary condition was water elevation, recomputed at every time step assuming normal flow conditions. The simulations started with a plane channel bed and continued until the bed topography stabilized, at least partly.

2.2. Computational Results

[25] Rapidly growing and relatively short alternate bars developed first. Subsequently, bar wavelength gradually increased and bar celerity gradually decreased, similar to the bar development simulated by *Nelson* [1990] using another nonlinear model. Eventually nonmigrating bars evolved slowly. The time needed to produce nonmigrating bars depended on the sediment transport capacity of the flow and on the imposed upstream boundary conditions. This was reflected in the different durations of the computations. The permanent upstream perturbation produced the fastest stabilization of a nonmigrating-bar pattern, with bars starting immediately at the perturbed upstream boundary. Without this permanent upstream perturbation, nonmigrating bars

Table 3. Numerical Parameters of Model Setup

Parameter	Value
Grid cell size in transverse direction (m)	15
Grid cell size in longitudinal direction (m)	25
Time step (minutes hydrodynamic simulated time)	0.5
Morphological factor[a]	10

[a]Multiplication factor of bed level changes to speed up the computations.

developed more slowly and only beyond a certain distance from the upstream boundary. This distance implies that the bars were not caused by imperfections in the uniformity of the inflow conditions.

[26] We can exclude the presence of any significant (reflection) effects from the downstream boundary, since the bars that were migrating in downstream direction could disappear from the computational field with neither geometrical deformations nor changes in celerity when approaching the downstream boundary.

[27] The longitudinal bar wavelengths were derived by means of spectral analyses, using a Fast Fourier Transform (FFT) program. The results of the spectral analyses always showed one or two clearly dominating spectral density peaks. Tables 4 and 5 give the wavelengths of the two highest peaks at different times.

[28] The longitudinal bed level profiles of RUN1, 15 m from the right bank, are shown in Figures 2 and 3 for the three boundary conditions. Figure 2 shows the longitudinal near-bank profiles after 2 and 4 simulated years. Figure 3 shows the bed topography at the moment in which the bed was either fully stable, i.e., contained only nonmigrating bars, or only partly stable, at the end of computations. The long computational time was the only reason to stop the computations when the bed was not completely stable yet.

[29] The bar celerity was roughly estimated by recording bar top locations at different times. In the first phases of the evolution, celerities had the order of magnitude of hundreds of meters per year, i.e., several times the channel width per year. At the final stages, they became of the order of meters per year or less, i.e., a hundredth part of a channel width per year.

[30] Given the large wavelengths and considering the overestimation of bar celerity caused by the morphological factor, bars having celerity of a few meters per year can be reasonably considered nonmigrating. The averaged values of the bar celerity computed for either the upstream or the downstream half of the channel were used to assess whether bars started to stabilize from upstream or from downstream (Table 6). Bars became nonmigrating either from upstream or downstream.

[31] Figures 4 and 5, show that the bar wavelengths increased with time until they reached an equilibrium value. In RUN 1, the final steady bar wavelengths were 10.6 to 11.7 times the channel width; 11.1 to 12.1 times in RUN 2. On average, the final steady bar wavelength was 11.4 times the channel width. The difference in final bar wavelength between the three cases having different boundary conditions was less than 10%.

3. Long-Duration Flume Experiment

3.1. Experimental Setup

[32] The experiment focused on the formation of bars, migrating and nonmigrating, in a straight channel at nonresonant conditions, either with a permanent upstream flow perturbation or without any perturbations. The experiment consisted of recording the long-term water flow and channel bed evolution in a straight flume with sand bed, fixed banks, and constant discharge (Figure 1, left).

[33] The total length of the flume was 26 m, but because of the measuring and postprocessing techniques the effective length became 20 m; the channel width was 60 cm. The bed was covered by an initially smooth layer of sand having a thickness of 25 cm. The median diameter of the sediment D_{50} was 0.238 mm. Water and sediment were recirculated, but water was added regularly, to compensate for small losses because of evaporation. The discharge was kept at 6.9 L/s.

[34] A wire mesh was introduced at the upstream boundary to dissipate the excess energy of the incoming water and to distribute the flow uniformly. A honeycomb flow straightener was placed immediately downstream of it, followed by a floating sponge to further diminish large-scale fluctuations and to suppress surface waves.

[35] Because of the presence of dunes and ripples, the rough data had to be filtered to clean the bar signal. The filter used was based on the Matlab software ProcessV3 and optimized for bed forms having wavelength larger than 1 m (bars). The characteristics of migrating bars were determined by plotting subsequent filtered bed level profiles, which allowed detecting their size and celerity. Nonmigrating bars were identified by averaging the filtered bed level profiles over time, which smoothed out most unsteady signals. Unfortunately, the filtering and time averaging reduced the amplitude of the bar signal. Upstream turbulence and perturbation smoothing as well as the measuring

Table 4. RUN1: Bar Wave Lengths Corresponding to the Highest Two Peaks Resulting from the Spectral Analysis at Different Times[a]

Morphological Simulated Time (year)	Groyne		Max Random Perturbation 1%		Max Random Perturbation 5%	
	First Peak	Second Peak	First Peak	Second Peak	First Peak	Second Peak
2	907	453	798	384	Only small bed oscillations	Only small bed oscillations
4	907	453	997	767	950	767
8	907	453	798	384	831	998
12	907	475	798	384	867[b]	-
16	950	475	798	997	867	623
20	950	475	798	867	731	383
28	950	475	907	998	1050[b]	-
36	950	475	907	391	1108[b]	-
42	950	475	907[a]	-	1050[b]	-
54	950	475	950[a]	-	1050[b]	-

[a]Bar wave lengths are given in meters.
[b]The *s* peak from spectral analysis very small or absent.

Table 5. RUN2: Bar Wave Lengths Corresponding to the Highest Two Peaks Resulting from the Spectral Analysis at Different Times[a]

Morphological Simulated Time (yr)	Groyne		Max Random Perturbation 1%		Max Random Perturbation 5%	
	First Peak	Second Peak	First Peak	Second Peak	First Peak	Second Peak
2	1050	525	867[b]	-	1050	512
4	907	453	1174	907	1050	512
8	1663	1425	1247	1425	1425	1174
12	1535	2850	1535	3325	1425	1663
16	1535	2850	1663	3325	1535	798
20	1663	2494	1663	2850	1535	1814
28	1663[b]	-	1814[b]	-	1663	1425
36	1814[b]	-	1663	1425	Run stopped after 28 yr	Run stopped after 28 yr
42	1814[b]	-	1663	1425	Run stopped after 28 yr	Run stopped after 28 yr

[a]Bar wave lengths are in meters.
[b]The *s* peak from spectral analysis very small or absent.

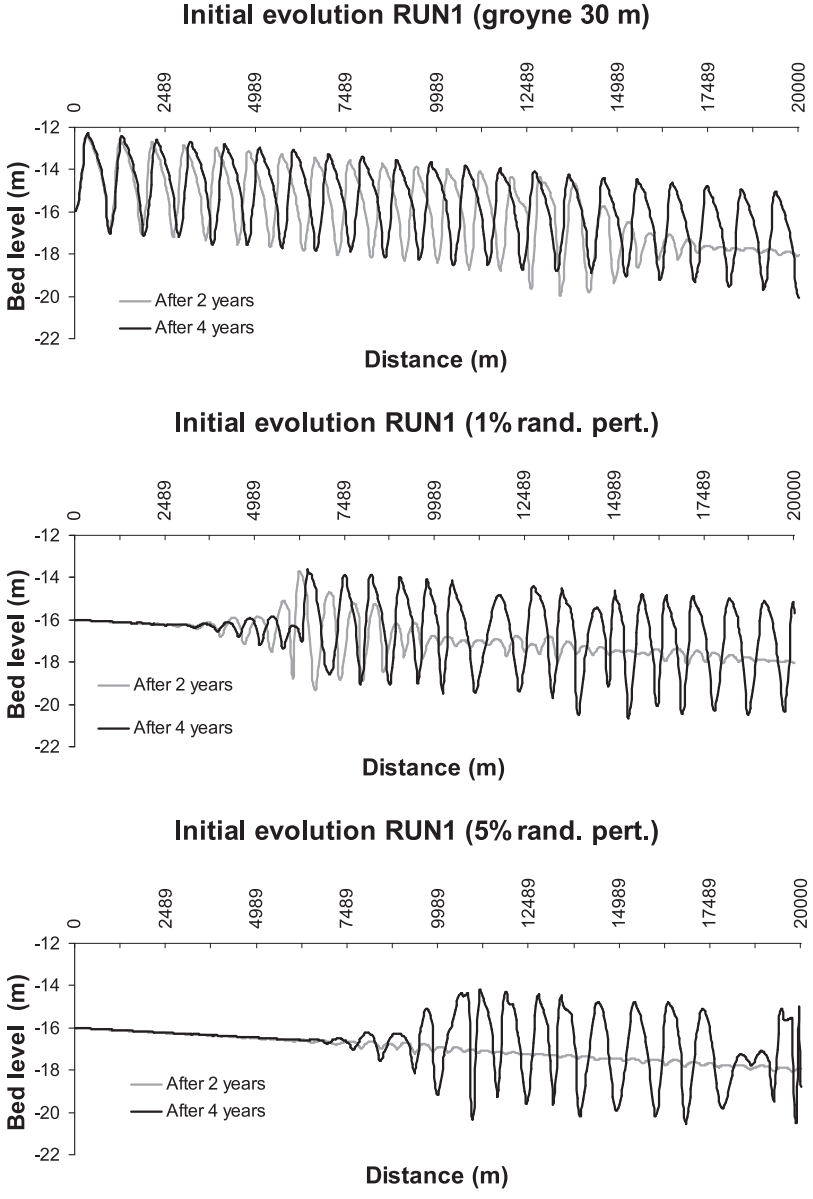

Figure 2. RUN1: initial longitudinal bed level profiles at 15 m from the left bank after 2 years (continuous line) and after 4 years (dotted line) from the start of the simulation.

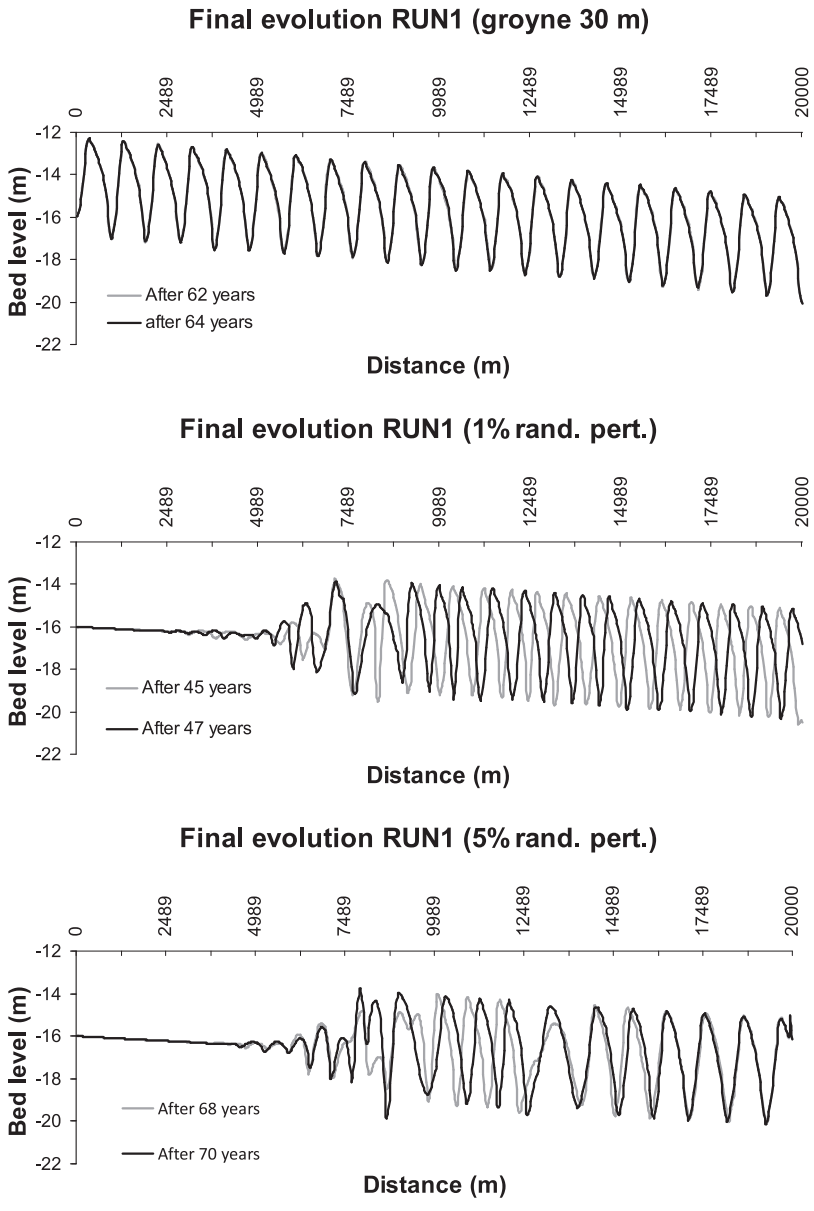

Figure 3. RUN1: longitudinal bed level profiles at 15 m from the left bank when the channel bed was either fully stabilized or had started to stabilize.

and postprocessing techniques adopted reduced the effective length of the channel to about 20 m.

[36] We could not carry out any spectral analyses, since the length of the flume was only 2–3 times the steady bar wavelength. In such cases, spectral peak locations are too dependent on initial phase. Some tentative FFT runs produced indeed unacceptable results.

[37] Two experimental tests were carried out. In the first one, a transverse plate was placed at the upstream boundary to create a permanent external flow perturbation. This test

Table 6. Averaged Bar Celerity in the Upstream and Downstream Half of the Channel (Total Length 20 km) at the Final Stage of Computations[a]

	Groyne		Max random pert. 1%		Max random pert. 5%	
Run	First 10 km	Second 10 km	First 10 km	Second 10 km	First 10 km	Second 10 km
RUN1	0.5	0.8	153.7[b]	125[b]	50	2.5
RUN2	28.7	2.9	1.4	3.9	40	2

[a]Half of the channel was a total length of 20 km. The Averaged bar celerity is in m/y.
[b]The run was stopped when only a few bars had become nonmigrating. These nonmigrating bars cannot be recognized from the average value of bar celerity computed over a 10 km long reach.

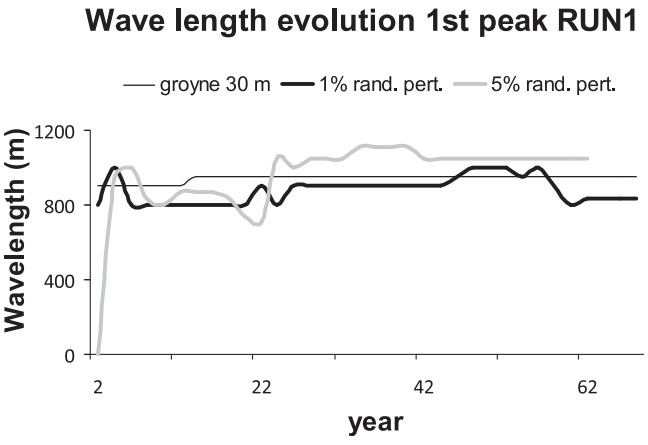

Figure 4. RUN 1: results of spectral analysis. Temporal evolution of the first-peak alternate-bar wavelength.

was meant to study the formation of nonmigrating bars in a reference case similar to previous experiments [*Struiksma and Crosato*, 1989; *Lanzoni* 2000a, 2000b]. These bars are generally referred to as "forced" bars, since they represent the free river response to finite external forcing. In the second test, the transverse plate was removed and the initial bed carefully smoothed out to eliminate all perturbations to the flow. The second test was meant to study the evolution of the bed topography in the same system, but without any external forcing. Previous experimental tests [e.g., *Fujita and Muramoto*, 1985] would suggest that this case would lead to the formation of migrating bars only.

3.2. Test With External Forcing

[38] The experiment with a transverse plate started on 11 June 2009 with the layout shown in Figure 6. Overall morphodynamic equilibrium, characterized by a constant longitudinal slope, was reached within 2 days. At that point, the flow characteristics were those listed in Table 7.

[39] The value of the damping coefficient and the wavelength of nonmigrating bars, computed using equations (2) and (6), respectively, assuming $b = 5$ and $E = 0.5$, are $1/L_D = -0.12$ (m^{-1}) and $L_P = 4.9$ m. The negative damping coefficient implies that the experimental conditions were super-resonant.

[40] Longitudinal profiles of the bed and water levels were measured three times per day. Transverse velocity profiles were measured across several sections, but less frequently.

[41] Nonmigrating alternate bars started to develop immediately after the start of the experiment, forced by the presence of the plate. Their wavelength slowly increased from an initial value of 6.5 m to a final value of about 7.5 m, reached after about 2 weeks. The initial and final values of bar wavelength were 10.8 and 12.5 times the channel width, respectively. Figure 7 shows the temporal evolution of the relative longitudinal bed level profile measured 5 cm from the left sidewall. Each curve plotted in Figure 7 represents the bed level profile averaged over one week. Time averaging smoothed out most of the migrating bars. Two and a half nonmigrating bars became visible.

[42] Relatively short migrating bars were present from the first day on, but only in the second half of the flume (Figure 8). The area in which migrating bars developed gradually reduced in size, moving downstream. This was because of the gradual dominance of nonmigrating bars, starting from upstream.

[43] The typical wavelength of migrating bars ranged between 2.6 and 4.1 m. These wavelengths were 4.3 to 6.8 times the channel width, one third to one half of the steady bar wavelength, as observed also in previous experiments [e.g., *Lanzoni*, 2000a]. The bar celerity ranged between 22 and 39 cm/h; the (filtered) bar amplitude between 5 and 17 mm.

3.3. Test Without External Forcing

[44] The experiment without external forcing started on 30 June 2009, and its duration was about 10 weeks, which is much longer than the duration of any other published experiment of this type. Overall morphodynamic equilibrium, characterized by a constant longitudinal slope, was reached within 2 days. Since that moment, the flow characteristics were those listed in Table 8. The small differences in the values of longitudinal slope, water depth, and flow velocity with respect to the previous experiment can be

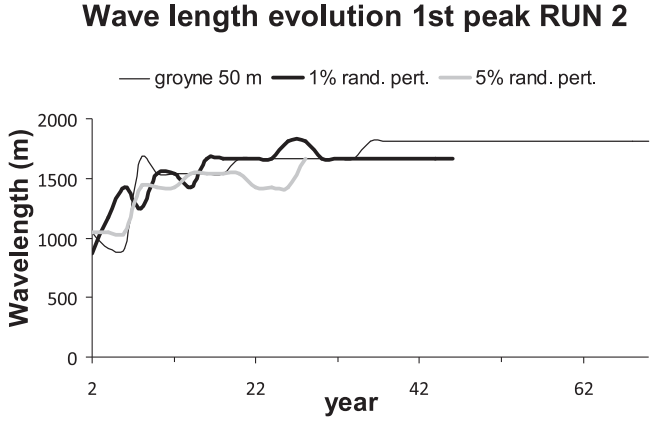

Figure 5. RUN 2: results of spectral analysis. Temporal evolution of the first-peak alternate-bar wavelength.

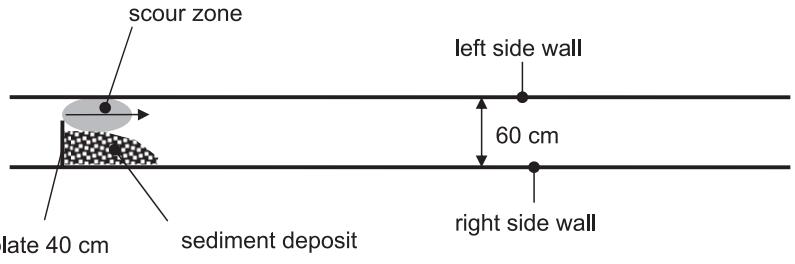

Figure 6. Flume with a transverse plate partially obstructing the inflow.

attributed to the absence of the transverse plate, which caused extra resistance in the preceding test.

[45] The value of the damping coefficient and the wavelength of nonmigrating bars, computed using equations (2) and (6), assuming $b = 5$ and E = 0.5, were $1/L_D = -0.08$ (m^{-1}) and $L_P = 5.1$ m. This means that the conditions were again super resonant.

[46] Transverse profiles of depth-averaged flow velocity were measured at 2.2, 12.2, and 22.2 m from the upstream boundary, twice per day for the first 10 days and once every 3 days during the month July. The time-averaged values of flow velocity near the upstream boundary did not show deviations from uniformity. This excluded the presence of any external forcing caused by inflow nonuniformities.

[47] During the first week, the longitudinal profiles of bed and water levels were measured 3 times per day. These measurements were subsequently carried out twice per day in July and only once every 3 days in August. At the end of August the measurements were carried out again with the initial frequency.

[48] On 5 September, 68 days after the start, an accident occurred to the pump which compromised the progressive bed evolution. The last useful measurement was taken on 4 September.

[49] A single (weak) nonmigrating alternate bar started to appear in the upstream half of the flume already 1 day after the start of the experiment. However, during the first weeks this bar had small amplitude and was unstable, since it disappeared and reappeared at the same place several times. The initial wavelength of this nonmigrating bar was about 7.0 m. Just like in the previous experiment, the wavelength gradually increased. The final value of approximately 7.5 m was reached about 3 weeks after the start of the experiment. Subsequently, the nonmigrating bar grew slightly in amplitude and two more bars started to appear. These became visible, although not well developed, about 6 weeks after the start of the experiment. Figure 9 shows the longitudinal profile of the time-averaged bed elevation along the left sidewall. The gray line represents the average of the first month and the black line the average of the second month of the experiment.

[50] Unfortunately the experiment had to be stopped when the nonmigrating bars were still in development, which means that we cannot show the completion of the bar growth process. Nevertheless, Figure 9 clearly shows the nonmigrating waving bed topography.

[51] The time-averaged values of the bed level profiles measured along both left and right sidewalls are plotted in Figure 10. Shallow areas near one sidewall correspond to pools near the opposite sidewall. This demonstrates that the bed oscillation is because of the presence of nonmigrating alternate bars.

[52] The nonmigrating bars have a different phase lag than in the preceding test with external forcing and smaller amplitude, but they have the same wavelength. This allows the conclusion that the nonmigrating bars that developed during the test without forcing are of the same type as the traditional "forced" bars. This is in line with the numerical results in section 2.

[53] Migrating bars started to form from the first day on. Their wavelength ranged between 2.5 and 4.9 m; their celerity between 23 and 40 cm/h; their (filtered) amplitude between 5 and 16 mm. Migrating bars were initially present along most of the flume length, but once nonmigrating bar started to appear, migrating bars formed only in the second half of the flume (Figure 11). The situation became similar to the one in the preceding test with the transverse plate, which means that, even in the absence of any upstream disturbance, the channel bed topography gradually acquired the characteristics of a "forced" system.

4. Discussion

[54] Our findings shed a new light on previous experiments in which nonmigrating bars appeared but were ascribed to imperfections in the experimental setup rather than to an intrinsic instability. *Crosato* [2008] reports that her 1989 reference experiment without upstream perturbation [*Struiksma and Crosato*, 1989] exhibited a nonmigrating bed deformation, despite many efforts to make the inflow conditions perfectly uniform. *Lanzoni* [2000a] obtained a simultaneous occurrence of alternate bars with two different wavelengths, one about twice as long as the other one, in his experimental tests P2403 and P0404 for uniform sediment. There were no evident upstream perturbations. Bars with different wavelengths occurred simultaneously also in *Lanzoni*'s [2000b] experiments with graded sediment. Our

Table 7. Experimental Conditions at Reach-Scale Equilibrium, Test With Transverse Plate

Channel Length (m)	Channel Width (m)	Longitudinal Bed Slope (-)	Water Discharge (m^3/s)	Mean Sed. Diameter (mmol)	Mean Water Depth (m)	Mean Flow Velocity (m/s)
26	0.6	3.54 ‰	6.9×10^{-3}	0.238	0.051	0.225

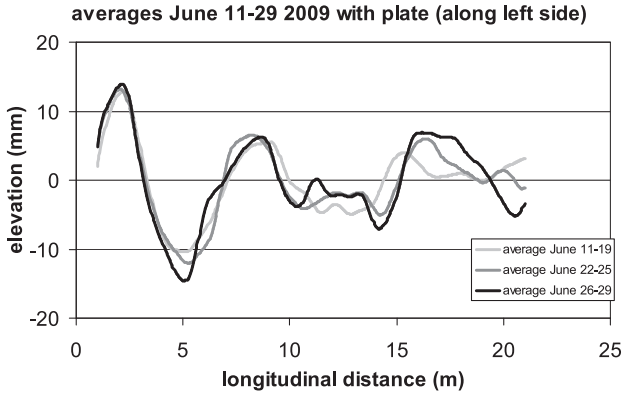

Figure 7. Weekly averaged bed level profiles measured at 5 cm from the left sidewall (values relative to the cross-sectionally averaged value of the bed level). Test with transverse plate.

findings suggest that the slow development of nonmigrating bars in the absence of a substantial steady upstream perturbation explains why they remained unnoticed in previous experiments and numerical studies of migrating alternate bars. Apparently, previous experiments and computations had been terminated before completion of the transition process from migrating to nonmigrating bars. The fastest growing bars characterize a transient stage rather than the final channel bed topography.

[55] *Struiksma and Crosato*'s [1989] experiments, *Lanzoni*'s [2000a, 2000b] experiments, and the present work relate to straight channels with nonerodible banks. The initiation of meandering in situations with erodible banks can be studied from the milestone experiments by *Friedkin* [1945]. He reproduced the initiation and progression of river meandering in the absence of upstream perturbations and sediment feeding with a constant discharge. He documented the vertical and lateral movement of an initially straight trapezoidal channel during an experimental run of 72 h. In the experiment, the channel was allowed to widen in a 40 m long and 12 m wide basin filled with fine sand characterized by a median diameter D_{50} equal to 0.20 mm, whereas the diameter for which 90% of the material is smaller, D_{90}, was 0.26 mm. The channel was exposed to a constant discharge of 8.5 L/s. Figure 12 shows the initial and final conditions. During the experimental test, the channel width increased and, because of the increase of channel sinuosity, the longitudinal bed slope decreased. The averaged initial and final channel characteristics are listed in Table 9. We derived the values of the variables not given directly by Friedkin from the pictures provided and from the assumption that the Chézy coefficient did not change with time.

[56] Friedkin did not provide information on the formation of alternate bars during the experiment, but *Rüther and Olsen*'s [2007] numerical simulation of this experiment shows that alternate bar formation preceded the initiation of meandering and that meanders developed from upstream to downstream. Table 10 lists the nonmigrating bar characteristics at the initial and final stages, computed using equations (2) and (6) with the adoption of *Engelund and Hansen*'s [1967] transport formula ($b = 5$) and $E = 0.5$ in equation (5). The spatial damping coefficient was negative both at the start and at the end of the experiment. The onset of meandering in Friedkin's experiment is hence related to neither resonance nor the intrinsic nonmigrating bars identified in straight channels with nonerodible banks. Initial localized bank erosion because of migrating bars appears to be the main mechanism.

[57] The intrinsic nonmigrating bars in straight channels with nonerodible banks still lack a theoretical explanation. The marginally stable nonmigrating bars of *Struiksma et al.* [1985] and *Seminara and Tubino* [1992] imply that nonmigrating bars are part of the natural response, but they do not explain why this part becomes dominant in the absence of steady perturbations or resonant conditions. Once present, nonmigrating bars might suppress migrating bars in the same way as *Tubino and Seminara*'s [1990] suppression of migrating bars by point bars in sinuous channels, but this still does not explain the initial growth of nonmigrating bars. Our first hunch is that the unsteadiness introduced by the mere presence of migrating bars might excite a steady

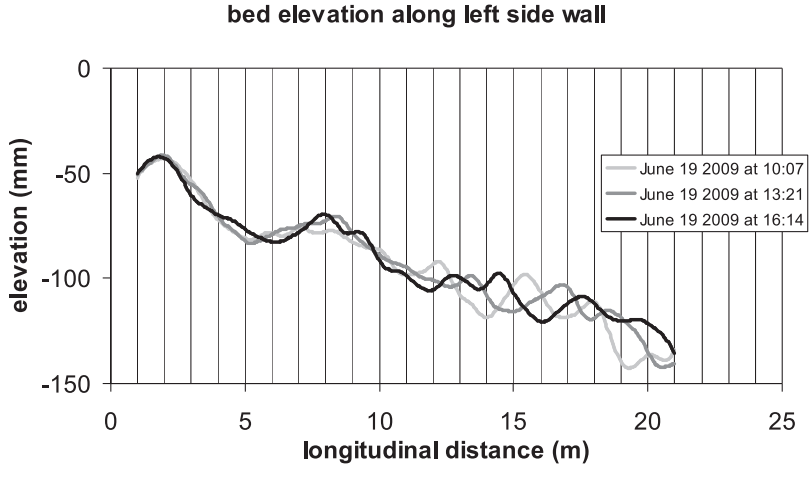

Figure 8. Successive measurements of bed level profile at 5 cm from the left sidewall (filtered data). Test with transverse plate.

Table 8. Experimental Conditions at Reach-Scale Equilibrium, Test Without Transverse Plate

Channel Length (m)	Channel Width (m)	Longitudinal Bed Slope (-)	Water Discharge (m^3/s)	Mean Sed. Diameter (mmol)	Mean Water Depth (m)	Mean Flow Velocity (m/s)
26	0.6	3.74 ‰	6.9×10^{-3}	0.238	0.049	0.235

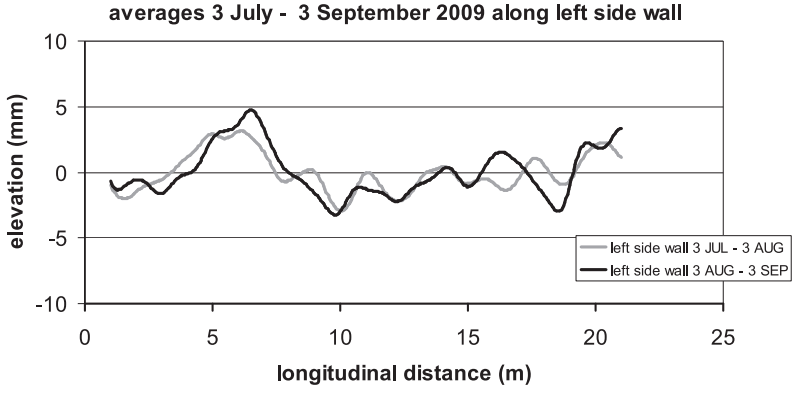

Figure 9. Monthly averaged longitudinal profiles of bed elevation at 5 cm from the left sidewall (values relative to the cross-sectionally averaged value of the bed level). Test without transverse plate.

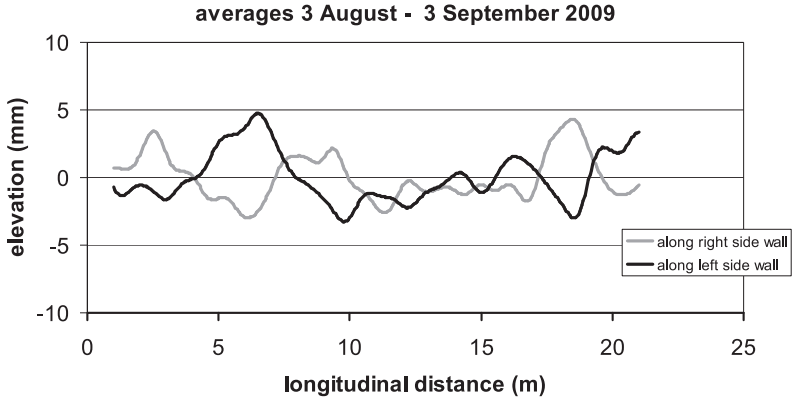

Figure 10. Monthly averaged longitudinal profiles of bed elevation at 5 cm from the left and right sidewalls (values relative to the cross-sectionally averaged value of the bed level). Test without transverse plate.

mode in the response. *Mosselman*'s [2009] crude analysis to demonstrate this, however, has been criticized (G. Seminara, personal communication, 2009), because he introduces temporal variations of bar wavelength at the end of the mathematical derivation instead of including them from the start.

[58] The results of this study, applied only to sand-bed channels, do not allow determining in which cases nonmigrating bars form spontaneously or not. We believe, however, that they arise when the river conditions fall within the range of steady bar formation defined by *Struiksma et al.* [1985], i.e., when the solution of equation (6) is real, but extra work would be needed to confirm this.

5. Conclusions

[59] We carried out 2-D numerical computations and a long-duration mobile-bed flume experiment to investigate the hypothesis that nonmigrating bars might be an intrinsic response of alluvial channel beds in straight channels. The numerical computations were carried out with a physics-based depth-averaged morphological model. Here short migrating alternate bars developed first, but slowly growing, nonmigrating bars, characterized by larger wavelengths, evolved subsequently, starting from either upstream or downstream. The nonmigrating bars dominated the final bed topography, notwithstanding the absence of resonant conditions, nonuniformities in the inflow conditions, or reflections

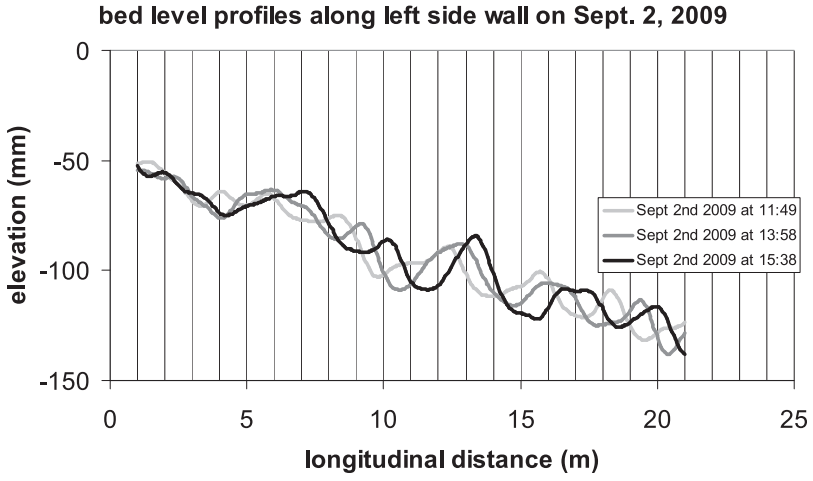

Figure 11. Successive measurements of bed level profile at 5 cm from the left sidewall (filtered data). Test without transverse plate.

from the downstream boundary. Migrating bars developed first in the flume experiments too. In the test without external forcing, the first nonmigrating bar stabilized its length about three weeks after the start of the experiment. Subsequently, this bar grew slightly in amplitude and two more nonmigrating bars became visible about 6 weeks after the start of the experiment. Apparently, fast growing migrating bars represent a transient stage and are not representative for the final channel bed topography.

[60] We reviewed earlier experiments on migrating alternate bars by *Struiksma and Crosato* [1989] and *Lanzoni* [2000a, 2000b] where either a steady oscillation (reported by *Crosato* [2008]) or bars with a similar wavelength as nonmigrating bars had been observed. Our findings suggest that these could be nonmigrating bars that were an intrinsic response rather than a response forced by imperfections in the uniformity of the inflow conditions, as thought previously.

[61] As nonmigrating bars are seen as a key ingredient in explanations of river meandering, we also reviewed *Friedkin*'s [1945] mobile-bed experiments with erodible banks. Here meanders developed without a steady upstream perturbation or resonant conditions, but *Rüther and Olsen*'s [2007] simulation suggests that initial localized bank

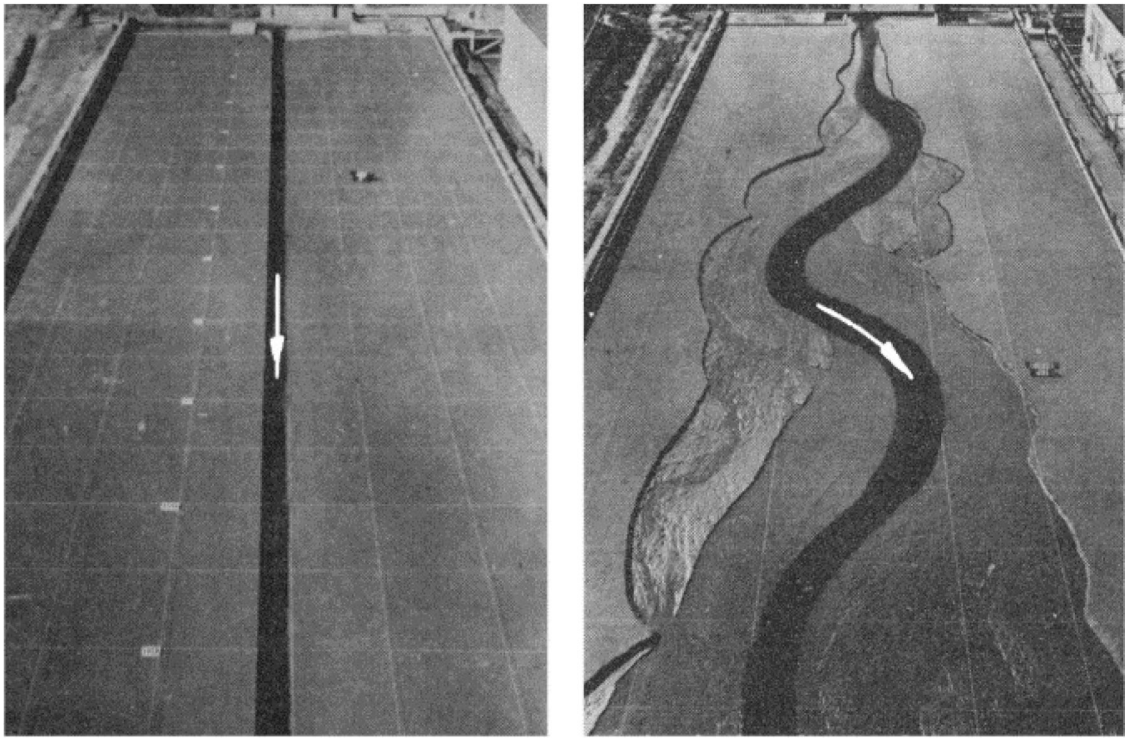

Figure 12. *Friedkin* [1945]: meander evolution at super-resonant conditions without any appreciable upstream disturbance.

Table 9. Initial and Final Channel Characteristics *Friedkin's* [1945] Experiment (Plate 2)

Friedkin [1945]	Q (m^3/s)	B (m)	S (-)	D_{50} (m)	h_0 (m)	u_0 (m/s)	B/h_0 (-)
Initial	0.0085	0.6	0.009	0.0002	0.05[b]	0.31[b]	12[b]
Final	0.0085	1.0[a]	0.007[a]	0.0002	0.04[a]	0.24[b]	25[b]

[a]Derived from the picture.
[b]Computed.

Table 10. Computed Nonmigrating Bar Characteristics at Initial and Final Stages of *Friedkin's* [1945] Experiment[a]

Friedkin [1945]	b (-)	λ_W (m)	λ_S (m)	L_P (m)	$1/L_D$ (1/m)
Initial	5	0.53	0.75	4.03	−0.28
Final	5	0.41	2.09	13.83	−0.98

[a]The experiment is on plate 2.

erosion because of migrating alternate bars triggered this development.

[62] We conclude that both nonmigrating alternate bars in straight channels with nonerodible banks and incipient meanders in straight channels with erodible banks can be intrinsic responses of an alluvial channel bed that do not require resonant conditions or an imposed steady upstream perturbation. However, the nature of the two intrinsic responses is different. The nonmigrating bars between nonerodible banks result from the slow development of a marginally stable nonmigrating bed topography mode. Meanders and associated nonmigrating bars between erodible banks are generated by localized bank erosion at the initial pools of migrating alternate bars. For erodible but very resistant banks, however, the slow development of intrinsic nonmigrating bars may still become the main mechanism for incipient meandering in conditions without resonance or imposed steady perturbations.

[63] **Acknowledgments.** This research has been granted by the Water Research Centre Delft. We thank Nigel Wright and Salomon Kroonenberg for encouraging us to investigate the onset of river meandering. We thank Jonathan Nelson and Huib De Vriend for the fruitful discussions, and Giampaolo Di Silvio for his constructive feedback that significantly contributed to improve our work. We thank Mick Van Der Wegen for his helpful advices in the modeling phase and Ulysse Le and Ayalew Abate Getaneth for their help in the measurements.

References

Bagnold, R. A. (1966), An approach to the sediment transport problem from general physics, *U.S. Geol. Survey Pap.*, 422-I, p. 37.

Blanckaert, K., L. Glasson, H. R. A. Jagers, and C. J. Sloff (2003), Quasi-3D simulation of flow in sharp open-channel bends with equilibrium bed topography, in *River, Coastal and Estuarine Morphodynamics: RCEM* 2003, vol. 1, edited by A. Sánchez-Arcilla and A. Bateman, pp. 652–663, IAHR, Madrid.

Blondeaux, P., and G. Seminara (1985), A unified bar-bend theory of river meanders, *J. Fluid Mech.*, *157*, 449–470.

Callander, R. A. (1969), Instability and river channels, *J. Fluid Mech.*, *36*(3), 465–480.

Crosato, A. (2008), Analysis and modelling of river meandering, Ph.D. Thesis, 251 p., Delft Univ. of Technol., Delft, Netherlands.

Crosato, A., and E. Mosselman (2009), Simple physics-based predictor for the number of river bars and the transition between meandering and braiding, *Water Resour. Res.*, *45*, W03424, doi:10.1029/2008WR007242.

De Vriend, H. J., and N. Struiksma (1984), Flow and bed deformation in river bends, in *River Meandering*, Proceedings of the Conference on Rivers'83, edited by C. M. Elliott, pp. 810–828, Am. Soc. of Civ. Eng., New York.

Einstein, A. (1926), Die Ursache der Mäanderbildung der Flussläufe und des sogenannten Baerschen Gesetzes (in German), *Naturwissenschaften*, *11*, 223–224.

Engelund, F., and E. Hansen (1967), A monograph on sediment transport in alluvial streams, Dan. Tech. Press. Copenhagen.

Engelund, F., and O. Skovgaard (1973), On the origin of meandering and braiding in alluvial streams, *J. Fluid Mech.*, *57*(2), 289–302.

Fredsøe, J. (1978), Meandering and braiding of rivers, *J. Fluid Mech.*, *84*(4), 609–624.

Friedkin, J. F. (1945), A laboratory study of the meandering of alluvial rivers, U.S. Army Eng. Waterw. Exp. St., Vicksburg, Miss.

Fujita, Y., and Y. Muramoto (1982), Experimental study on stream channel processes in alluvial rivers, *Bull. Disaster Prev. Res. Inst., Kyoto Univ.*, *32*(1), 49–96.

Fujita, Y., and Y. Muramoto (1985), Studies on the process of development of alternate bars, *Bull. Disaster Prev. Res. Inst., Kyoto Univ.*, *35*(3), 55–86.

Hall, P. (2004), Alternating bar instabilities in unsteady channel flows over erodible beds, *J. Fluid Mech.*, *499*, 49–73.

Hansen, E. (1967), On the formation of meanders as a stability problem, *Prog. Rep. 13*, 9 p., Coastal Eng. Lab., Tech. Univ. Den.

Ikeda, S. (1982), Lateral bed slope transport on side slopes, *J. Hydraul. Div.*, *108*(11), 1369–1373.

Ikeda, S., G. Parker, and K. Sawai (1981), Bend theory of river meanders, Part 1: Linear development, *J. Fluid Mech.*, *112*, 363–377.

Kinoshita, R., and H. Miwa (1974), River channel formation which prevents downstream translation of transverse bars, *Shin Sabo, Engl. Transl.*, *94*, 12–17.

Lanzoni, S. (2000a), Experiments on bar formation in a straight flume: 1. Uniform sediment, *Water Resour. Res.*, *36*(11), 3337–3349.

Lanzoni, S. (2000b), Experiments on bar formation in a straight flume: 2. Graded sediment, *Water Resour. Res.*, *36*(11), 3351–3363.

Lebreton, J. C. (1974), *Dynamique Fluviale* (in French), Collection de la Direction des Etudes et Recherches d'Electricité de France, Eyrolles, France.

Lesser, G. R., J. A. Roelvink, J. A. T. M. Van Kester, and G. S. Stelling (2004), Development and validation of a three dimensional morphological model, *Coastal Eng.*, *51*(8–9), 883–915.

Lisle, T. E., H. Ikeda, and F. Iseya (1991), Formation of stationary alternate bars in a steep channel with mixed-side sediment: a flume experiment, *Earth Surf. Proc. Landforms*, *16*, 463–469.

Macagno, E. O. (1989), Leonardian fluid mechanics in the Manuscript I, *IIHR Monogr. 111*, Iowa Inst. of Hydraul. Res., Univ. of Iowa, Iowa City, Iowa.

Marra, W. A. (2008), Dynamics and interactions of bars in rivers and the relation between bars and a braided river pattern, B.Sc. Thesis, Fac. of Geosci., Dept. of Phys. Geogr., Utrecht Univ., Utrecht, Netherlands.

Mosselman, E. (2005), Basic equations for sediment transport in CFD for fluvial morphodynamics, in *Computational Fluid Dynamics; Applications in Environmental Hydraulics*, edited by P. D. Bates, S. N. Lane, and R. I. Ferguson, chap. 4, pp. 71–89, Wiley, New York.

Mosselman, E. (2009), Intrinsic steady alternate bars in alluvial channels. Part 2: Theoretical analysis, in *Proceedings of the 6th Symposium on River Coastal and Estuarine Morphodynamics (RCEM 2009)*, vol. 2, pp. 767–772, Taylor and Francis, New York.

Mosselman, E., K. I. Hassan, and A. Sieben (2003), Effect of spatial grain size variations in two-dimensional morphological computations with uniform sediment, in *Proceedings IAHR Symposium River, Coastal and Estuarine Morphodynamics*, edited by A. Sánchez-Arcilla and A. Bateman, pp. 236–246, Int. Assoc. for Hydro-Environ. Eng. and Res., Madrid.

Nelson, J. M. (1990), The initial stability and finite-amplitude stability of alternate bars in straight channels, *Earth Sci. Rev.*, *29*(1–4), 97–115, doi:10.1016/0012-8252(90)90030-Y.

Nelson, J. M., and J. D. Smith (1989), Evolution and stability of erodible channel beds, in *River Meandering*, edited by S. Ikeda and G. Parker, *Water Resour. Monogr.*, vol. 12, pp. 321–377, AGU, Washington, D. C.

Olesen, K. W. (1984), Alternate bars in and meandering of alluvial rivers, in *River Meandering*, edited by C. M. Elliott, pp. 873–884, Am. Soc. of Civ. Eng., New York.

Parker, G. (1976), On the cause and characteristic scales of meandering and braiding in rivers, *J. Fluid Mech.*, *76*(3), 457–479.

Parker, G., and H. Johannesson (1989), Observations on several recent theories of resonance and overdeepening in meandering channels, in *River Meandering*, edited by S. Ikeda and G. Parker, *Water Resour. Monogr.*, vol. 12, pp. 379–415, AGU, Washington, D. C.

Rhoads, B. L., and M. R. Welford (1991), Initiation of river meandering, *Prog. Phys. Geogr.*, *15*(2), 127–156.

Rüther, N., and N. R. B. Olsen (2007), Modelling free-forming meander evolution in a laboratory channel using three-dimensional computational fluid dynamics, *Geomorphology*, *89*, 308–319.

Seminara, G., and M. Tubino (1992), Weakly nonlinear theory of regular meanders, *J. Fluid Mech.*, *224*, 257–288.

Struiksma, N. (1998), Test computations with Delft 2D-Rivers, *Rep. 9.6600*, Delft Hydraul., Delft, Netherlands.

Struiksma, N., and A. Crosato (1989), Analysis of a 2 D bed topography model for Rivers, in *River Meandering*, edited by S. Ikeda and G. Parker, *Water Resour. Monogr.*, vol. 12, pp. 153–180, AGU, Washington, D. C.

Struiksma, N., K. W. Olesen, C. Flokstra, and H. J. De Vriend (1985), Bed deformation in curved alluvial channels, *J. Hydraul. Res.*, *23*(1), 57–79.

Talmon, A. M., N. Struiksma, and M. C. L. M. van Mierlo (1995), Laboratory measurements of the direction of sediment transport on transverse alluvial-bed slopes, *J. Hydraul. Res.*, *33*(4), 495–517.

Tubino, M., and G. Seminara (1990), Free-forced interactions in developing meanders and suppression of free bars, *J. Fluid Mech.*, *214*, 131–159.

F. Beidmariam Desta, Ethiopian Road Authority, P.O. Box 1770, Addis Ababa.

A. Crosato, E. Mosselman, Section of Hydraulic Engineering, Faculty of Civil Engineering and Geosciences, Delft University of Technology, Stevinweg 1, 2628 CN Delft, Netherlands. (a.crosato@tudelft.nl)

W. S. J. Uijttewaal, Section of Fluid Mechanics, Faculty of Civil Engineering and Geosciences, Delft University of Technology, Stevinweg 1, 2628 CN Delft, Netherlands.